

# Ferromagnetic resonance study of diluted Fe nanogranular films

Satoshi Tomita<sup>a)</sup>

*PRESTO, Japan Science and Technology Agency (JST), Wako, Saitama 351-0198, Japan*

Masayuki Hagiwara and Takanari Kashiwagi

*Magnetic Materials Laboratory, RIKEN (The Institute of Physical and Chemical Research), Wako, Saitama 351-0198, and Graduate School of Integrated Science, Yokohama City University, Tsurumi, Yokohama 230-0045, Japan*

Chusei Tsuruta and Yoshio Matsui

*National Institute for Materials Science (NIMS), Namiki, Tsukuba 305-0044, Japan*

Minoru Fujii and Shinji Hayashi

*Department of Electrical and Electronics Engineering, Faculty of Engineering, Kobe University, Nada, Kobe 657-8501, Japan*

(Received 5 January 2004; accepted 23 March 2004)

Ferromagnetic resonance (FMR) in diluted Fe nanogranular films with low volume fractions of Fe ( $v$ ) has been studied. Films prepared by a co-sputtering technique are composed of amorphous Fe nanoparticles embedded in SiO<sub>2</sub> glass matrices. The resonance of the FMR uniform mode is found to be strongly affected by the  $v$ , the temperature, and the angle between the film plane and the applied magnetic field. The present study suggests that the values of these parameters should be carefully selected in order to realize left-handed materials using diluted ferromagnetic-metal nanogranular films. © 2004 American Institute of Physics. [DOI: 10.1063/1.1739526]

## I. INTRODUCTION

Films consisting of ferromagnetic-metal nanoparticles embedded in nonmagnetic matrices are known as ferromagnetic-metal nanogranular films. The structure of the nanogranular films can be specified by the volume fraction of the magnetic granules ( $v$ ). In the range of  $v = 50$ – $60\%$  the nanometer-size granules are in close contact with each other (structural percolation threshold  $v_p$ ), forming infinite networks of “wormy” textures.<sup>1</sup> Just below the  $v_p$ , ferromagnetic-metal nanoparticles in the films are closely packed and separated by very thin nonmagnetic layers. Such films have been intensively studied as promising materials for use in magnetic data storage media with ultra-high recording density.<sup>2–5</sup>

In contrast to the “dense” ferromagnetic-metal nanogranular films, “diluted” films with very low  $v$ , in which the ferromagnetic-metal granules are completely isolated by matrices, have received little attention. Diluted ferromagnetic-metal nanogranular films are, however, of interest for realizing left-handed materials (LHMs)<sup>6</sup> having simultaneously negative electrical permittivity ( $\epsilon$ ) and negative magnetic permeability ( $\mu$ ) in the microwave region.<sup>7</sup> This is based on the fact that  $\mu$  of ferromagnetic materials for electromagnetic waves can be negative in the vicinity of the ferromagnetic resonance (FMR) frequency, which is usually in the microwave region.<sup>8,9</sup> In order to realize LHMs by this approach, detailed knowledge of FMR conditions in the nanogranular films is necessary.

In this paper, we have reported the results of FMR studies of diluted Fe nanogranular films with small values for the

Fe volume fraction ( $v$ ). The experimental procedures are briefly summarized in the following section (Sec. II). Section III is devoted to the characterization of film composition and structure, and to FMR studies as a function of the  $v$ , the temperature, and the angle between an applied magnetic field and the film plane. Finally, in Sec. IV we conclude the paper.

## II. EXPERIMENTAL

Nanogranular Fe-SiO<sub>2</sub> films were prepared by a co-sputtering technique. Fe chips were placed on a SiO<sub>2</sub> target. They were simultaneously sputtered in 2.7 Pa Ar gas using a rf magnetron sputtering apparatus. This technique enables a small volume fraction of Fe in the films to be controlled by the areal ratio of Fe and SiO<sub>2</sub> on the sputtering target. Films about 10  $\mu\text{m}$  in thickness were deposited onto quartz substrates for FMR studies. The substrates were not heated during the deposition. The as-deposited films were studied.

The volume fraction in the films was estimated by using electron probe microanalyses (EPMA). The EPMA were carried out on films 1  $\mu\text{m}$  in thickness deposited on Al plates. A cross section of the samples was observed using a transmission electron microscope (TEM) operated at 800 kV. The specimens for the TEM observations were prepared according to standard procedures including mechanical and Ar-ion thinning techniques.

FMR studies were performed using a conventional X-band ( $\nu = 9.1$  GHz) ESR spectrometer equipped with a cylindrical TE<sub>011</sub> cavity. The samples (about 3 mm  $\times$  3 mm) were placed onto a quartz sample holder, put into the cavity, and held in either parallel or perpendicular orientation to the sample plane of the applied magnetic field. FMR spectra were obtained by sweeping the magnetic field from 0 to 10

<sup>a)</sup>Electronic mail: s-tomita@riken.go.jp

kOe. The magnetic field was calibrated using a  $\alpha$ ,  $\alpha$ -diphenyl- $\beta$ -picryl hydrazyl (DPPH) sample ( $g=2.0036$ ). A standard field modulation technique was used so that the detected signal corresponded to the first field derivative of the absorbed microwave power. A He gas-flow cryostat combined with a temperature controller allowed us to vary the sample temperature continuously in the range of 3–300 K. In addition to FMR studies, the magnetization of the samples on various temperatures and magnetic fields was investigated using a superconducting quantum interference device (SQUID) magnetometer.

### III. RESULTS AND DISCUSSION

#### A. Film composition and structure

In this study, EPMA was used to determine the ratio of the atomic concentrations of Fe to Si ( $X_{\text{Fe}}/X_{\text{Si}}$ ). The volume fraction of Fe [ $v$  (%)] was then calculated from the atomic Fe:Si ratio using  $v/(100-v)=0.260(X_{\text{Fe}}/X_{\text{Si}})$ .<sup>10</sup> This relation assumes that the material is completely phase-separated into  $\text{SiO}_2$  and crystalline  $\alpha$ -Fe. On the other hand, Fe nanoparticles have amorphous structures in the present samples, as will become obvious later. Therefore,  $v$  calculated in this manner does not give a strictly correct volume fraction of Fe in the films. Since this slight difference was not thought to seriously affect the conclusions, the calculated  $v$  was used to keep our notation consistent with that used by others. Though Fe nanogranular films have been prepared with  $v=1, 5, 15, 20$ , and 24%, the  $v=5\%$  and 15% films are the focus of this study.

Figure 1 shows a cross-sectional TEM image of a film with  $v=15\%$ . Spherical dark patches about 2 nm in diameter can be seen. These patches correspond to Fe nanoparticles in amorphous  $\text{SiO}_2$  matrices. The micrograph shows no obvious evidence of physically connected particles. As shown in the inset, the size distribution of the particles is narrow. The average diameter ( $d_{\text{ave}}$ ) and standard deviation ( $\sigma$ ) are 2.01 nm and 0.42 nm, respectively. Debye–Scherrer rings in a selected-area electron diffraction (SAED) pattern are quite broad (not shown here). Almost all of the rings were assigned to amorphous Fe,<sup>11</sup> although a few dim rings could not be identified. Based on these findings, the  $v=15\%$  film was characterized by isolated, roughly spherical, and amorphous Fe nanoparticles with  $d_{\text{ave}}=2.01$  nm embedded in  $\text{SiO}_2$  glass matrices. TEM observation of another film with  $v=5\%$  also revealed that amorphous Fe nanoparticles about 1 nm in diameter were dispersed in the  $\text{SiO}_2$  glass matrices.

TEM studies have indicated that Fe nanoparticles in the films possess amorphous rather than crystalline structures. The formation of amorphous Fe nanoparticles in as-deposited Fe– $\text{SiO}_2$  films prepared by a co-sputtering method was previously reported by Holtz *et al.*<sup>10</sup> They reported that sputtered films had an excess of silicon; the O:Si atomic ratio was less than 2.0. The excess silicon atoms incorporated into the Fe particles were considered responsible for the amorphous phase of Fe. It was also reported that post-deposition annealing between 480–700 °C under vacuum converts the particles from amorphous to crystalline.

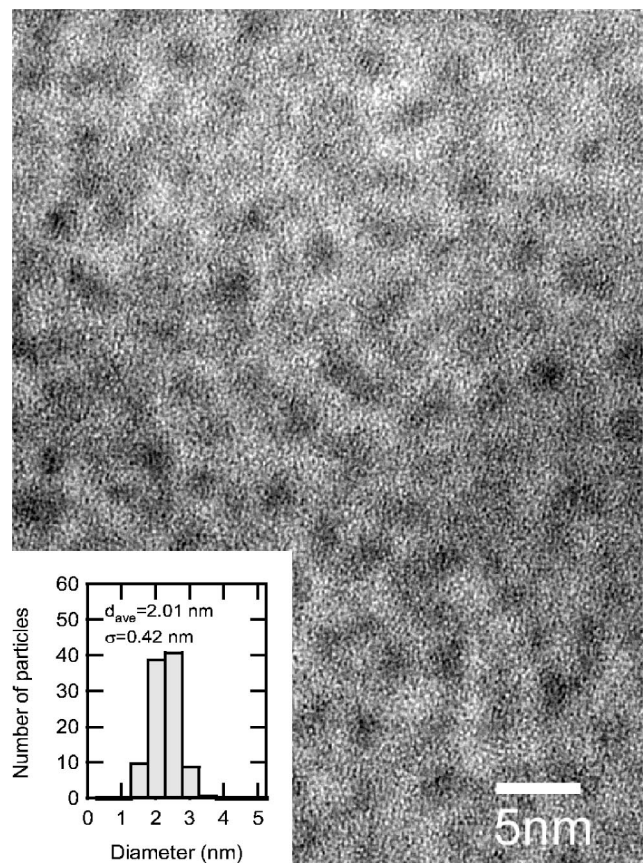


FIG. 1. A cross-sectional TEM image of a film with  $v=15\%$ . The inset shows the size distribution of the particles.

#### B. Ferromagnetic resonance studies

Figures 2(a) and 2(b) show the FMR spectra obtained at room temperature for films with  $v=5$  and 15%, respectively. Note that the spectra correspond to the field derivative of the absorbed microwave power. The inset of Fig. 2(a) illustrates the configuration of a sample in an applied magnetic field ( $H$ ). The  $\theta$  was defined as the angle between  $H$  and the film plane;  $\theta=0^\circ$  and  $\theta=90^\circ$  correspond to  $H$  in the directions parallel and perpendicular to the film plane, respectively.

In Fig. 2(a), a broad resonance at about 3000 Oe could be clearly observed. The  $g$  value of this resonance is about 2.20. This resonance signal is referred to as the main resonance signal in the following. In addition to the main resonance signal, a weak signal around 500 Oe was observed. The origin of this weak signal has yet to be elucidated. Figure 2(a) shows that the position and width of the main resonance signal for the  $v=5\%$  film are independent of  $\theta$ . On the other hand, the resonance signal for the film with  $v=15\%$  was influenced by  $\theta$  [Fig. 2(b)]. At  $\theta=0^\circ$ , the signal appeared around 2900 Oe (solid line), whereas the signal appeared upfield at 3500 Oe for  $\theta=90^\circ$  (dashed line).

More detailed FMR studies were carried out by changing the temperature in the range of 4–300 K. It should be first noted that the position of the signal in the film with  $v=5\%$  was almost entirely independent of the temperature. Thus, only the results for the film with  $v=15\%$  are shown in Fig. 3. Figure 3(a) shows the temperature dependence of the

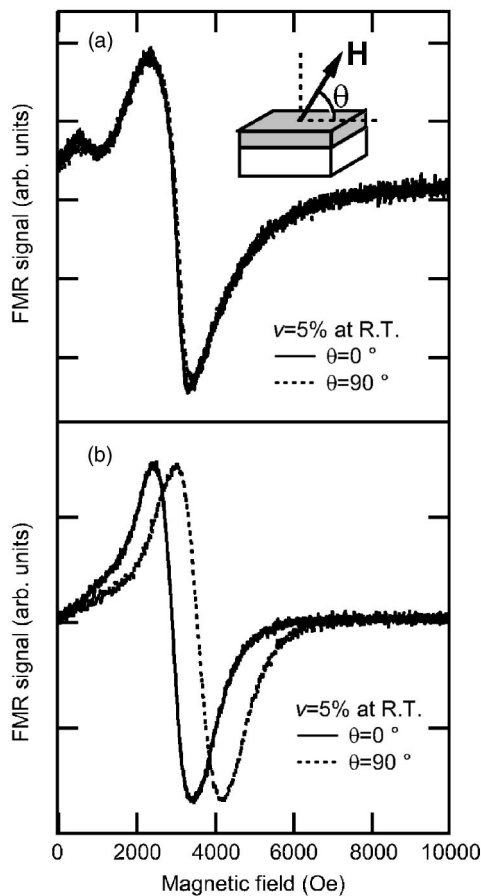


FIG. 2. Room temperature FMR spectra of films with (a)  $v=5\%$  and (b)  $v=15\%$ . The inset illustrates the configuration of a sample and an applied magnetic field.

FMR spectrum at  $\theta=0^\circ$ . Suppression of the signal intensity in the vicinity of the zero field at low temperatures is an artifact caused by a magnet power supply. The main resonance signal appeared around 2900 Oe at room temperature. As the temperature decreased, the resonance signal was ob-

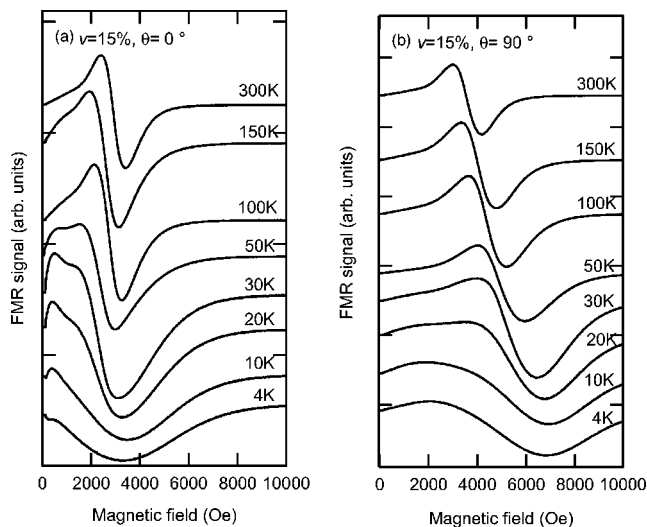


FIG. 3. The temperature dependence of FMR spectra for a film with  $v=15\%$  at (a)  $\theta=0^\circ$  (the parallel configuration) and (b)  $\theta=90^\circ$  (the perpendicular configuration).

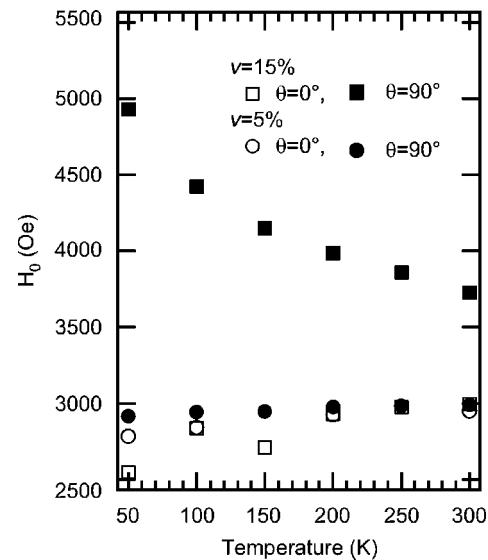


FIG. 4. The resonance field of the main-resonance ( $H_0$ ) in films with  $v=5\%$  ( $\circ, \bullet$ ) and in  $v=15\%$  ( $\square, \blacksquare$ ) are plotted as a function of temperature down to 50 K. The open and solid marks correspond to the  $H_0$  in the parallel and perpendicular configurations, respectively.

served to broaden and shift to a lower magnetic field. Figure 3(b) shows the temperature variation of the spectra at  $\theta=90^\circ$ . The main resonance signal shifted towards a higher field and broadened with decreasing temperature.

In addition to the main resonance signal in Fig. 3(a) below 150 K, another signal was observed at a lower field, around 1000 Oe, and was remarkable at around 30 K. Also at  $\theta=90^\circ$  [Fig. 3(b)], a broad signal around 2000 Oe was observed at low temperatures. The position of the signal in both configurations shifted to a slightly lower field as the temperature decreased. A similar feature was observed by Sharma and Baiker<sup>12</sup> in FMR spectra for a silica-supported Ni catalyst (Ni content 8%). One of the possible origins of this subsidiary feature is unsaturation of the magnetization of the films.<sup>13</sup> The deformation of the main resonance signal due to the appearance of this subsidiary feature is thus believed to be prevented in a high field, in other words, in a high frequency FMR study.

### C. Main resonance signal in FMR spectra

In Fig. 4, the resonance field for the main resonance ( $H_0$ ) in the film with  $v=15\%$  is plotted as a function of temperature. The open and solid squares correspond to  $H_0$  at  $\theta=0^\circ$  and  $\theta=90^\circ$ , respectively. In an effort to derive  $H_0$ , data analyses were conducted. The derivative FMR spectrum was integrated to obtain a spectrum of absorbed microwave power, and the spectrum was then decomposed into two signals with Lorentzian lineshapes. The  $H_0$  was derived from the decomposed signal at a higher field. It was very difficult to decompose the spectra well at low temperatures due to the broadness and deformation, thus only the data from room temperature to 50 K were presented.

The  $H_0$  of the signal for the  $v=15\%$  film at  $\theta=90^\circ$  (the solid squares in Fig. 4) appeared at about 3700 Oe at room temperature and shifted upfield upon cooling. It finally

reached about 5000 Oe at 50 K. On the other hand, the  $H_0$  at  $\theta=0^\circ$  (open squares) shifted from about 3000 Oe to the downfield as the temperature decreased. The results for the  $v=5\%$  film at  $\theta=0^\circ$  (open circles) and at  $\theta=90^\circ$  (solid circles) are also shown in the same figure for comparison. The  $H_0$  of the  $v=5\%$  film was observed to be independent of both the angle and the temperature.

It should be mentioned here that both the  $v=5\%$  and 15% films showed spontaneous magnetization in the M–H curves obtained by the SQUID magnetometer, although the data is not shown here. The spontaneous magnetization is believed to originate from ferromagnetic amorphous Fe nanoparticles in the films.<sup>14</sup> It is thus reasonable to interpret the main resonance signals as due to a FMR uniform mode (the Kittel mode<sup>9</sup>), which corresponds to a uniform precession of all of the magnetic moments coupled in the Fe nanoparticles with the angular frequency  $\omega_0$ . The FMR condition for an ellipsoidal ferromagnet, to which the external field is applied along the  $z$  axis, is given by the Kittel equation,<sup>9</sup>

$$\omega_0^2 = \gamma^2 [H_0 + (N_x - N_z)M_z][H_0 + (N_y - N_z)M_z], \quad (1)$$

where  $H_0$  is the applied magnetic field for the uniform mode resonance;  $M_z$  is the magnetization in the  $z$  direction; and  $\gamma$  is the gyromagnetic ratio, which is related to the  $g$  value by  $\gamma = -g\mu_B/\hbar$ . The Bohr magneton is represented by  $\mu_B$ , and  $\hbar$  is the Planck constant divided by  $2\pi$ . The  $N_x$ ,  $N_y$ , and  $N_z$  are the demagnetization factors along the  $x$ ,  $y$ , and  $z$  directions, respectively, which vary with the shape of the ferromagnet and satisfy the relation  $N_x + N_y + N_z = 4\pi$ . For a noninteracting uniform sphere, the shape effect can be neglected because  $N_x = N_y = N_z$ , and

$$\omega_0 / |\gamma| = H_0. \quad (2)$$

Equation (2) indicates that the  $H_0$  for magnetically isolated spherical magnets is independent of the magnetic field direction and temperatures below the Curie temperature. This clearly explains the angular and temperature dependence of the main resonance signal for  $v=5\%$ . Furthermore, the  $g$  factor of the signal ( $g=2.20$ ) is close to that of a uniform mode in bulk ferromagnetic Fe material, the value of which, obtained from the literature, is  $g=2.14 \pm 0.08$ .<sup>15</sup> The main resonance in  $v=5\%$  film can thus be assigned to a FMR uniform precession mode in the individual spherical Fe nanoparticle about 1 nm in diameter. This indicates that, in a film with  $v=5\%$ , the very small Fe nanoparticles are magnetically isolated and show superparamagnetism, in which the magnetic moment of each single domain nanomagnet is randomly oriented by thermal fluctuations.

An increase in  $v$  is followed by an increase in the size and density of Fe nanoparticles, as shown by the TEM observation. Superparamagnetic spherical Fe nanoparticles then begin to magnetically couple with each other at the magnetic percolation threshold ( $v_m$ ), resulting in the formation of magnetic networks in the films. Given that the ensemble of the coupled superparamagnetic moments above  $v_m$  behaves macroscopically as a thin magnetic film, a shape effect must be considered for FMR conditions. The Kittel equation [Eq. (1)] for ferromagnetic disks is expressed as

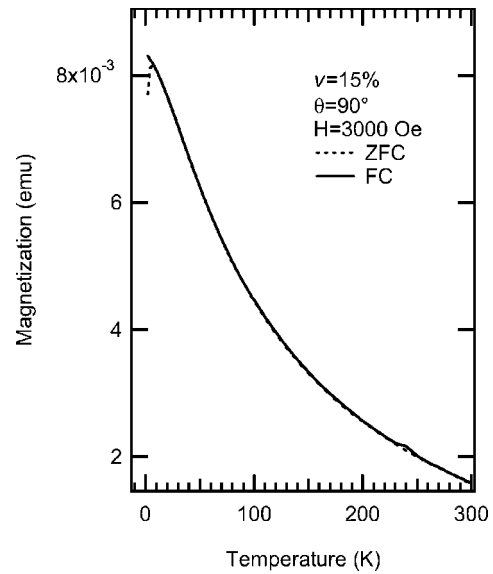


FIG. 5. Magnetization in  $v=15\%$  film at  $\theta=90^\circ$  during the zero-field-cooled (dashed line) and field-cooled (solid line) procedures under 3000 Oe.

$$\omega_0 / |\gamma| = \sqrt{H_0(H_0 + 4\pi M_z)}, \quad \theta=0^\circ, \quad (3a)$$

$$\omega_0 / |\gamma| = H_0 - 4\pi M_z, \quad \theta=90^\circ, \quad (3b)$$

where the term  $4\pi M_z$  represents the demagnetization effect. These equations suggest that the  $H_0$  in the parallel (perpendicular) configuration appears at a lower (higher) magnetic field than the resonance field without the demagnetization effect. The predicted angular dependence of the uniform mode signal is in good agreement with the present FMR results for  $v=15\%$  at room temperature; as shown in Fig. 4,  $H_0$  appeared around 3000 Oe at  $\theta=0^\circ$  and around 3700 Oe at  $\theta=90^\circ$ . These results clearly indicate that a film with  $v=15\%$  is beyond the magnetic percolation threshold  $v_m$ , and the amorphous Fe nanoparticles in the film are magnetically coupled despite the fact that  $v$  is low compared to that of the structural percolation threshold ( $v_p=50-60\%$ ). It is thus concluded that a slight difference in  $v$  affects the FMR conditions of diluted ferromagnetic-metal nanogranular films, and the permeability  $\mu$  of a film with  $v > v_m$  would exhibit anisotropy under a given magnetic field and microwave frequency.

Equations (3a) and (3b) also point out that the temperature dependence of  $H_0$  in a film with  $v=15\%$  is attributed to that of the  $4\pi M_z$ . The temperature dependence of  $M_z$  for  $v=15\%$  was investigated using a SQUID magnetometer. Figure 5 shows  $M_z$  versus temperature during zero-field-cooled (ZFC) and field-cooled (FC) procedures under a magnetic field of 3000 Oe. The dashed and solid lines correspond to ZFC and FC curves, respectively. The magnetic field was applied in the direction perpendicular to the film plane ( $\theta=90^\circ$ ). The ZFC curve indicates that the  $M_z$  has a peak at 6 K. This is attributed to the blocking phenomena of superparamagnetic particles.<sup>1</sup> As the temperature decreases, superparamagnetic particles of smaller and smaller size become successively blocked until the blocking temperature  $T_B$  of 6 K, where the ZFC curve shows a maximum. This blocking process leads to an increase in the  $M_z$  as the temperature

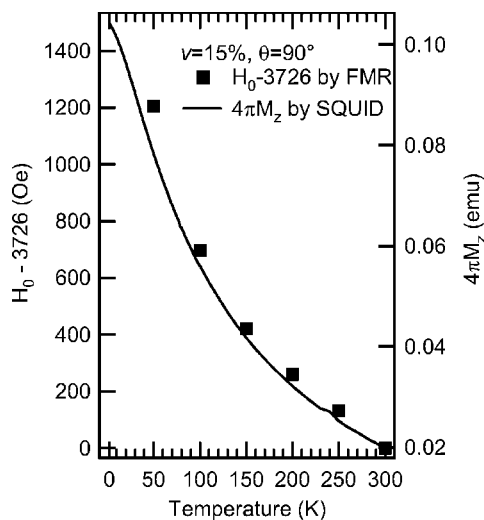


FIG. 6. The  $H_0 - 3726$  for  $v = 15\%$  film at  $\theta = 90^\circ$  derived from Fig. 4 and the  $4\pi M_z$  under 3000 Oe at  $\theta = 90^\circ$  derived from the FC curve in Fig. 5 are simultaneously plotted as a function of temperature.

decreases. Figure 6 shows the temperature dependence of the  $4\pi M_z$  derived from a FC curve in Fig. 5. In the same figure, the amount of the shift of the uniform mode signal for  $v = 15\%$  at  $\theta = 90^\circ$  ( $H_0 - 3726$ ) is plotted as a function of temperature (solid squares). The temperature dependence of the  $4\pi M_z$  is successful in qualitatively reproducing a shift of the resonance field  $H_0$ . This allows us to point out that the  $\mu$  of the film above  $v_m$  depends on the temperature at a given magnetic field and microwave frequency.

#### IV. CONCLUSIONS

FMR in diluted Fe nanogranular films with low volume fractions of Fe ( $v$ ) has been studied in detail as a function of the  $v$ , the temperature, and the angle between an applied magnetic field and the film plane. The results of  $v = 5$  and 15% films prepared by a co-sputtering method were presented. A clear resonance signal corresponding to the FMR uniform mode (the Kittel mode) was observed in both films. The two films showed completely different angular and temperature dependence of the resonance field. The uniform mode signal of the  $v = 5\%$  film was not affected by either the angle or the temperature of the film. On the other hand, the

signal of the  $v = 15\%$  film was found to strongly depend on the both these parameters. Even though the  $v = 15\%$  is far below the  $v$  value of the structural percolation threshold ( $v_p = 50 - 60\%$ ), this dependence can be explained by the Kittel equations for ferromagnetic disks, indicating that a film with  $v = 15\%$  is beyond the magnetic percolation threshold  $v_m$  and the ferromagnetic Fe nanoparticles in the film are magnetically coupled. The results suggest that a difference in  $v$ , the angle, and the temperature strongly affect the FMR conditions of diluted ferromagnetic-metal nanogranular films, i.e., these factors affect the permeability  $\mu$  of films under a given magnetic field and microwave frequency. In addition, the lower field side of the resonance signal with  $v = 15\%$  film was deformed probably due to unsaturation of the magnetization of the film. The unsaturation of the magnetization can be prevented by using a high magnetic field, in other words, in a high frequency FMR study above 10 GHz. The present study enables us to suggest that the  $v$ , angle, temperature, and operation frequency should be carefully selected in order to realize LHMs using diluted ferromagnetic-metal nanogranular films.

#### ACKNOWLEDGMENTS

The authors would like to acknowledge K. Toshikiyo, H. Yashiro, K. Katsumata, K. Takeuchi, and S. Ushioda for contributing a valuable discussion of this work.

- <sup>1</sup>C. L. Chien, J. Appl. Phys. **69**, 5267 (1991).
- <sup>2</sup>S. H. Liou and C. L. Chien, Appl. Phys. Lett. **52**, 512 (1988).
- <sup>3</sup>P. J. Grundy, J. Phys. D **31**, 2975 (1998).
- <sup>4</sup>R. L. Holtz, P. Lubitz, and A. S. Edelstein, Appl. Phys. Lett. **56**, 943 (1990).
- <sup>5</sup>A. Butera, J. N. Zhou, and J. A. Barnard, Phys. Rev. B **60**, 12270 (1999).
- <sup>6</sup>V. G. Veselago, Usp. Fiz. Nauk **92**, 517 (1964) [Sov. Phys. Usp. **10**, 509 (1968)].
- <sup>7</sup>S. T. Chui and L. Hu, Phys. Rev. B **65**, 144407 (2002).
- <sup>8</sup>S. Chikazumi, *Physics of Ferromagnetism* (Syokabo, Tokyo, 1984) (in Japanese).
- <sup>9</sup>C. Kittel, *Introduction to Solid State Physics*, 7th ed. (Wiley, New York, 1996).
- <sup>10</sup>R. L. Holtz, A. S. Edelstein, P. Lubitz, and C. R. Gossett, J. Appl. Phys. **64**, 4251 (1988).
- <sup>11</sup>T. Ichikawa, Phys. Status Solidi A **19**, 707 (1973).
- <sup>12</sup>V. K. Sharma and A. Baiker, J. Chem. Phys. **75**, 5596 (1981).
- <sup>13</sup>U. Wiedwald *et al.*, Phys. Rev. B **68**, 064424 (2003).
- <sup>14</sup>J. M. D. Coey, J. Appl. Phys. **49**, 1646 (1978).
- <sup>15</sup>A. F. Kip and R. D. Arnold, Phys. Rev. **75**, 1556 (1949).